

## REVIEW

[View Article Online](#)  
[View Journal](#) | [View Issue](#)



Cite this: *Chem. Sci.*, 2025, **16**, 5447

## Recent advances in room-temperature synthesis of covalent organic frameworks

Dongchuang Wu, <sup>\*a</sup> Ning Gu, <sup>a</sup> Junru Yao, <sup>a</sup> Yang Cao, <sup>b</sup> Lun Wang, <sup>b</sup> Imran Shakir, <sup>d</sup> Youyi Sun<sup>\*b</sup> and Yuxi Xu <sup>\*c</sup>

Covalent organic frameworks (COFs) have become a promising class of highly-crystalline polymers with layered stacking structures, ordered porous channels, and highly-tailorable structures. To date, most COFs have been synthesized *via* high-temperature solvothermal methods, which require complicated optimization of factors including temperature, solvent ratio, catalyst, and reaction time. Additionally, solvothermal conditions with high temperature and high pressure restrict the facile and large-scale synthesis of COFs for practical applications. In addition, the insolubility and lack of processability of the COF powders obtained *via* solvothermal methods hinder their potential application in film-related fields. Energy-efficient and environmentally benign synthetic methods to resolve these problems are highly desired. In this review, we provide an overview of the recent progress in room-temperature synthetic strategies for constructing COF powders or COF films. We first discuss *in situ* characterization technologies for exploring the COF growth mechanism. Then, we present representative room-temperature synthesis methods for COFs, including solid–liquid interfacial synthesis, liquid–liquid interfacial synthesis, on-water surface synthesis, water-phase synthesis, electrosynthesis, sonochemical synthesis, single-solution phase synthesis, mechanochemical synthesis, high-energy ionizing radiation synthesis, and photochemical synthesis. Finally, perspectives on room-temperature synthesis are proposed in the areas of single-crystal domains, novel room-temperature reaction types, crystallization mechanism, the design of chemical structures and green synthesis.

Received 7th January 2025

Accepted 6th March 2025

DOI: 10.1039/d5sc00109a

[rsc.li/chemical-science](http://rsc.li/chemical-science)

## 1. Introduction

Covalent organic frameworks (COFs) are a new class of highly crystalline organic polymers with highly adjustable structures and properties, in which the monomers and scaffolds are precisely arranged in two-dimensional (2D) or three-dimensional (3D) space.<sup>1</sup> The 2D layered COF structures are formed through van der Waals interactions between 2D planes. Dynamic covalent chemistry is considered to be the chemical basis by which the reversible chemical bonds can realize self-healing of internal defects in COF materials.<sup>2</sup> Recently, some irreversible reactions have also been used to synthesize COFs,<sup>3</sup> which requires more effort to be devoted to the structural design and the study of crystallization mechanism. However, to improve the crystallinity of COFs, tedious solvent screening, high reaction temperatures (>120 °C) and lengthy

polymerization times (>3 days) are always selected for the optimized solvothermal synthesis.<sup>4–6</sup> The resulting time-consuming and energy-intensive solvothermal syntheses make the large-scale production of COFs challenging.

In terms of determining the crystallization mechanism, the use of closed solvothermal reaction systems hinders *in situ* characterization of the dynamic process.<sup>7–9</sup> The heat source and sealed conditions limit the development of *in situ* monitoring equipment. Thus, in most reports involving new COF structures, solvothermal synthesis has been the first choice, and less attention has been paid to the crystallization mechanism.<sup>10–12</sup> Additionally, COFs synthesized by the solvothermal method are insoluble and unprocessable powders, which present formidable challenges in film-based applications.<sup>13–15</sup>

In the exploration of alternative synthetic approaches, the room-temperature synthesis of COFs has attracted increasing interest.<sup>16–18</sup> Compared with harsh solvothermal syntheses, room-temperature syntheses without a high-pressure environment feature mild reaction conditions, designable reaction systems, various assisted technologies and controllable reaction rate. Currently, various condensation reactions have been used to synthesize COFs at room temperature, such as the Suzuki coupling reaction, Schiff-base reaction, boronate ester condensation, Knoevenagel condensation, Mannich reaction,

<sup>a</sup>School of Energy and Power Engineering, North University of China, Taiyuan, 030051, China. E-mail: [wudongchuang@nuc.edu.cn](mailto:wudongchuang@nuc.edu.cn)

<sup>b</sup>School of Materials Science and Engineering, North University of China, Taiyuan 030051, China. E-mail: [syyi@pku.edu.cn](mailto:syyi@pku.edu.cn)

<sup>c</sup>School of Engineering, Westlake University, Hangzhou, 310024, China. E-mail: [xuyuxi@westlake.edu.cn](mailto:xuyuxi@westlake.edu.cn)

<sup>d</sup>Department of Physics, Faculty of Science, Sustainability Research Center, Islamic University of Madinah, Madinah 42351, Saudi Arabia



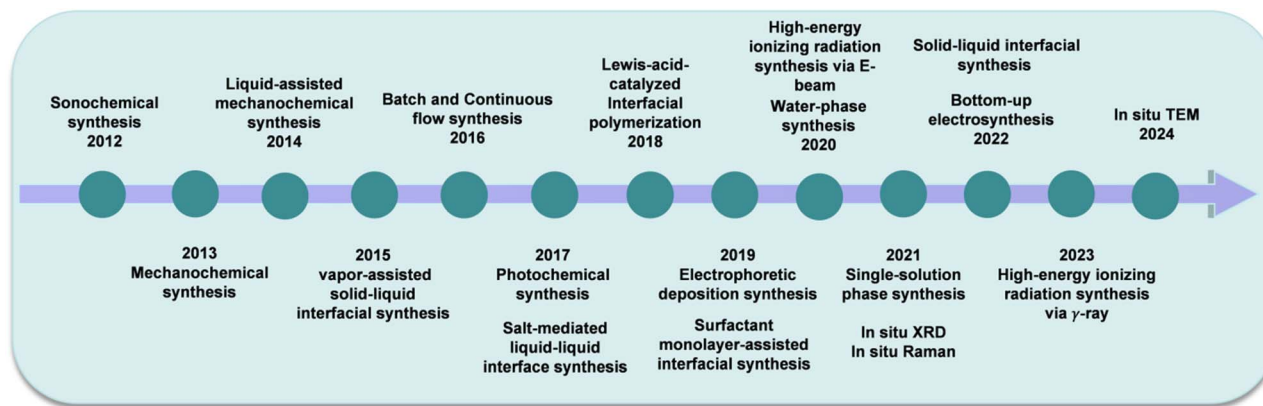


Fig. 1 Schematic presenting a timeline of the development of the room-temperature synthesis of COFs.

multicomponent reactions and imide reactions. In addition, unlike the polycrystalline products obtained *via* solvothermal syntheses, large-size single-crystal COFs can be prepared *via* low-temperature or room-temperature syntheses.<sup>19–21</sup> The growth of defects and single crystallinity can be well regulated and controlled *via* designed room-temperature syntheses.

In 2012, sonochemistry was first used for the rapid room-temperature synthesis of COFs. Subsequently, various advanced synthetic methods have been created for preparing COFs at room temperature. As shown in Fig. 1, in the last decade, various pioneering room-temperature synthetic strategies have been reported, such as solid–liquid interfacial synthesis, liquid–liquid interfacial synthesis, on-water surface synthesis, water-phase synthesis, electrosynthesis, sonochemical synthesis, single-solution phase synthesis, mechanochemical synthesis, high-energy ionizing radiation synthesis, and photochemical synthesis. In addition, to explore the crystallization mechanism, various *in situ* characterization technologies have been designed and used. In this review, with the aim of promoting innovations in the preparation of COF materials and their practical applications, a timely overview of the room-temperature synthesis of COFs is provided.

## 2. *In situ* characterization technologies for exploring the COF growth mechanism

The study of the crystallization mechanism of COFs is of great significance for developing new synthetic strategies. *Ex situ/in situ* characterization technologies have been used to investigate their growth mechanisms. Unlike *ex situ* characterization technologies for observing information after the experimental process, *in situ* characterization technologies can monitor the changes during the experimental process.<sup>22</sup>

### 2.1. IR spectroscopy

Infrared (IR) spectroscopy can record changes in the micro-environment and linkages *via* the location and intensity of the infrared absorption peaks of functional groups. *Ex/in situ* IR

spectroscopy can monitor the dynamic evolution of linkages during the synthesis of COFs. Banerjee and co-workers investigated the dynamic evolution of C=O and NH<sub>2</sub> groups *via* time-dependent IR during the covalent self-assembly of COF nanospheres (Fig. 2a).<sup>23</sup> Over 36 h, the –C=O peak at 1719 cm<sup>–1</sup> and two –NH<sub>2</sub> peaks at 3324 cm<sup>–1</sup> and 3354 cm<sup>–1</sup> of the COF nanospheres gradually disappeared in the time-dependent IR spectra of a TpAzo COF film, indicating the end of the covalent self-assembly.

### 2.2. Raman spectroscopy

Raman spectroscopy is typically used to determine the vibrational modes of molecules.<sup>24</sup> Raman spectroscopy and IR are complementary in the study of linkages.<sup>25</sup> COFs with symmetric molecular structures can be easily monitored using Raman techniques. Thus, the changes from disorder to order and the evolution from monomers to COFs can be detected using Raman spectroscopy. Recently, to investigate the evolution of linkages during mechanochemical synthesis, *in situ* Raman spectroscopy has been used to reveal the formation of C=N or boroxine ring linkages and the depletion of monomers.<sup>26,27</sup> As shown in Fig. 2b and c, Perepichka and co-workers provided the first *in situ* Raman spectroscopic insight into boronic acid condensation during the mechanochemical synthesis of COF-1; the peak intensity of the boroxine ring at 673 cm<sup>–1</sup> gradually increased as the boronic acid peak at 1100 cm<sup>–1</sup> gradually disappeared over the course of 3 h.<sup>26</sup>

### 2.3. X-ray diffraction

X-ray diffraction (XRD) is an important tool to study the structural information of crystals. The evolution of crystal faces can be detected *via* the location and intensity of the XRD peaks. Generally, *ex situ* XRD has been used to study the effects of different reaction conditions on the crystallinity. Recently, Lotsch and co-workers used *in situ* XRD and *in situ* Raman to monitor reaction intermediates during the mechanochemical synthesis of COF-LZU-1.<sup>28</sup> As shown in Fig. 2d and e, the XRD images of the intermediates were different from those of the monomers. Over the 50 min reaction, obvious strengthening of



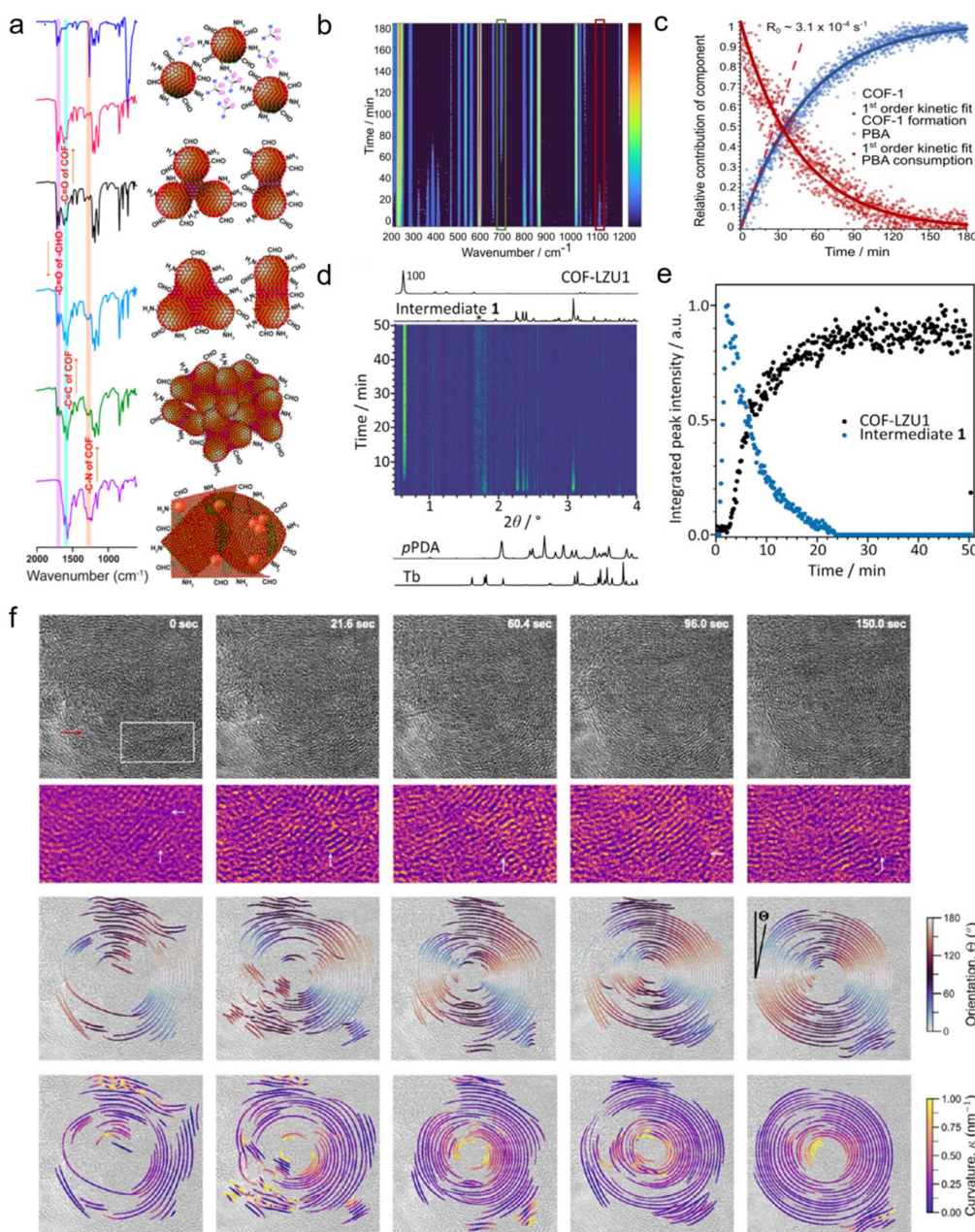


**Fig. 2** (a) Time-dependent IR of the formation of a COF film. Reproduced with permission from ref. 23. Copyright 2019 American Chemical Society. (b) *In situ* Raman spectroscopy during the synthesis of COF-1. (c) The scatter data of COF-1 and PDA. Reproduced with permission from ref. 26. Copyright 2024 Elsevier Ltd (d) 2D XRD plots during the mechanochemical reaction of COF-LZU1. (e) Normalized integrated peak intensities of COF-LZU1 and intermediates. Reproduced with permission from ref. 28. Copyright 2024 Wiley-VCH. (f) Real-time crystallization monitoring *via* *in situ* TEM during COF onion formation at 60 °C in liquid. Reproduced with permission from ref. 32. Copyright 2024 American Chemical Society.

the (100) plane of COF-LZU1 with decreasing intensity of intermediates were clearly observed. The *in situ* studies offered direct experimental evidence of 1,4-dioxane templating effects based on the observation of the solvated reaction intermediates.

#### 2.4. Microscopy

Microscopy technologies, including transmission electron microscopy (TEM) and scanning electron microscopy (SEM), can be used to observe morphological changes and crystalline

structure.<sup>29</sup> Due to the limitations of *in situ* reaction equipment, time-dependent *ex situ* TEM and SEM have typically been adopted by researchers to monitor morphology and structure.<sup>30,31</sup> Very recently, using *in situ* liquid-phase TEM, Zheng and co-workers elucidated the multistep pathways of COF onion nanostructure formation, as demonstrated in Fig. 2f. Real-time images acquired over 150 s *via* *in situ* TEM directly captured the graphitic layer formation, interlayer attachment, spacing relaxation, and structural homogenization.<sup>32</sup> The direct

evidence of crystallization provided unprecedented insights into the evolution of the crystallinity.

### 3. Room-temperature synthetic strategies for COFs

#### 3.1. Solid-liquid interfacial synthesis

In the last decade, substrate-assisted interface polymerization has been performed to synthesize COF films *via* high-temperature solvothermal methods.<sup>33</sup> However, the harsh reaction conditions and limited volume of the reaction vessel hinder the preparation of large-scale films and lower the film quality. Thus, the solid–liquid interface synthesis of COF films at room temperature, which can enhance the film quality by lowering the reversible reaction rate and achieve large-scale COF films using simple reaction equipment, has been explored.<sup>34,35</sup>

In 2015, Bein and co-workers developed a mild substrate- and vapor-assisted conversion for growing boronic-ester-linked COF films on glass substrates.<sup>36</sup> First, the COF precursors were dissolved in a polar solvent mixture. The mixture was then dripped onto a clean glass substrate. To ensure complete evaporation of the solvent, the wet glass substrate was placed in a desiccator containing methylene and dioxane (v/v = 1 : 1) at room temperature for 72 h. Finally, a dark green COF film was obtained on the glass. In addition, Lai and co-workers synthesized a highly crystalline COF film (COF-DT) at room temperature *via* placing an SiO<sub>2</sub>/Si substrate in a dilute precursor solution of 2,5-dihydroxy-1,4-phenyldialdehyde (DHTA) and 1,3,5-tri(4-aminophenyl)benzene (TAPB) for solid–liquid

interfacial growth.<sup>37</sup> As shown in Fig. 3a, the diluted solution allowed for slow nucleation and direct growth of the COF film. After 48 h, the SiO<sub>2</sub>/Si substrate was removed to obtain a COF-DT film, which was transferred to a PET carrier. Similarly, Chen and co-workers also reported *in situ* grown COF films *via* a solid–liquid interface in a dilute precursor solution.<sup>38</sup> The substrates were placed vertically into a precursor solution with a very low initial monomer concentration. As expected, heterogeneous nucleation occurred on the substrate surface. The *in situ* grown COF films had high crystallinity, uniform morphology and controllable thickness.

Interestingly, Banerjee and co-workers reported a novel residual crystallization (RC) method (Fig. 3b).<sup>39</sup> Different from the above method, a two-phase liquid–liquid system was designed, and the substrate was preplaced in the lower phase to form a solid–liquid interface. During the interfacial reactions, most of the crystallization reaction occurs at the liquid–liquid interface, and only a trace amount of residue crystallizes at the solid–liquid interface to form a COF film. The COF thin films synthesized *via* the RC method showcased high surface area, crystallinity, and conductivity at room temperature. A similar experimental method also was demonstrated by Alshareef and co-workers.<sup>40</sup>

#### 3.2. Liquid–liquid interfacial synthesis

Liquid–liquid interfacial synthesis requires a space-confined interface to grow 2D COF films. There are two general kinds of interfacial designs: (1) two kinds of monomers are dispersed in two different phases, which drives the dynamic reversible reaction to occur at the interface of the two phases. (2) The reactant and catalyst are dispersed in two different phases, ensuring that the catalytic reaction occurs between the two phases. The liquid–liquid interface is usually constructed using two immiscible liquids or two immiscible liquids plus a buffer interlayer, which confines the reactions to the 2D interface to form COF films. Common liquid–liquid two-phase interfaces include water/dichloromethane (DCM),<sup>30</sup> water/ionic liquid,<sup>41</sup> water/nitrobenzene<sup>42</sup> and water/ethyl acetate interfaces.<sup>43</sup>

In 2017, Banerjee and co-workers reported organic salt-mediated liquid–liquid interface synthesis technology, in which hydrogen bonding between an ammonium salt and water in aqueous solution can slow its diffusion rate; the slow interfacial diffusion rate drives the reaction in the direction of thermodynamically controlled crystallization (Fig. 4a).<sup>31</sup> Typically, 1,3,5-triformyl-phloroglucinol (Tp) was dissolved in DCM, and a water layer was then added on the DCM solution as a buffer layer to form a water/oil interface. An aqueous solution of dissolved aromatic amine-*p*-toluenesulfonic acid (PTSA) salts was slowly added to the buffer layer. After 72 h at room temperature, the self-supporting COF film was formed. Recently, Liu and co-workers reported the oil-in-water (O/W) emulsion interface-confined synthesis of imine-based 2D covalent organic frameworks (COFs) stabilized by cationic surfactants.<sup>44</sup> In addition to Schiff base reactions, the liquid–liquid interface technique can also be extended to the Suzuki coupling reaction<sup>45</sup> and Knoevenagel reaction.<sup>46</sup> In 2018, Li and co-

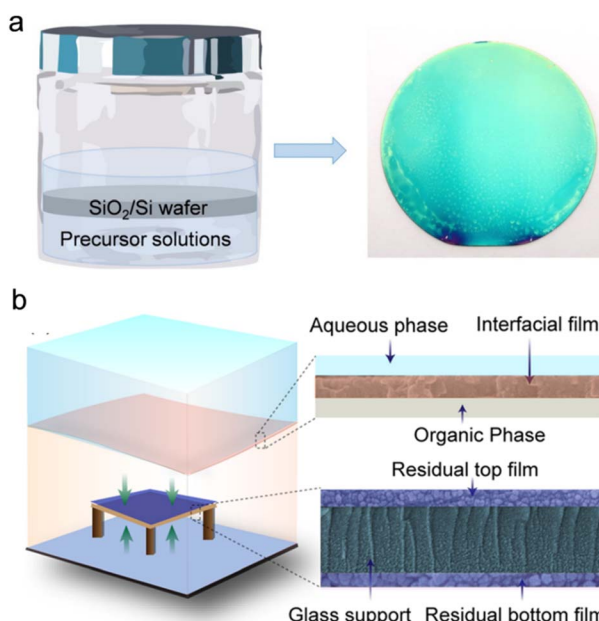


Fig. 3 (a) Solid–liquid interfacial synthesis of COF-DT films. Reproduced with permission from ref. 37. Copyright 2022 Wiley-VCH. (b) Fabrication of COF films at liquid–liquid and solid–liquid interfaces via interfacial and residual crystallization. Reproduced with permission from ref. 39. Copyright 2021 American Chemical Society.



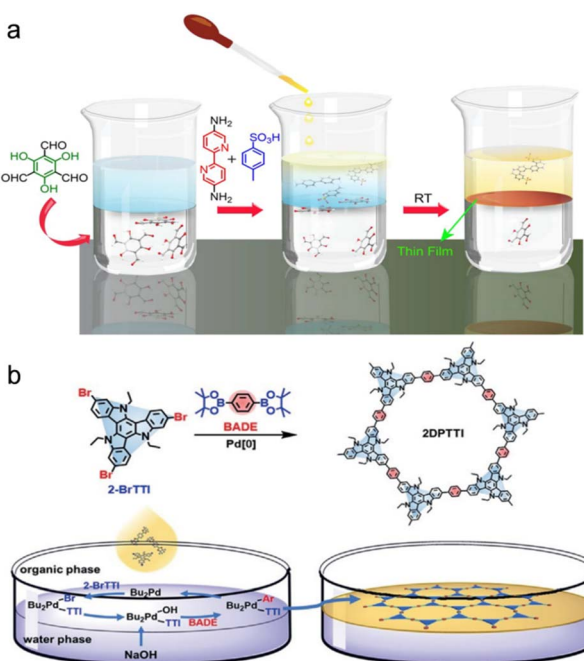


Fig. 4 (a) Schematic representation of the liquid–liquid interfacial crystallization process for synthesizing the Tp-Bpy thin film. Reproduced with permission from ref. 31. Copyright 2017 American Chemical Society. (b) Schematic of synthesis of a 2DPTTI film through a Suzuki reaction between the monomers 2-BrTTI and BADE. Reproduced with permission from ref. 47. Copyright 2020 Wiley-VCH.

workers synthesized carbon–carbon-bonded COF films through the Suzuki coupling reaction in a water/toluene two-phase system, in which the toluene phase contained reaction monomers and the catalyst  $\text{Pd}(\text{PPh}_3)_4$  was dropped on top of the  $\text{K}_2\text{CO}_3$  aqueous solution.<sup>45</sup> After a month of reaction in a 2 °C refrigerator under an argon atmosphere, 2D COF films with a large transverse size and crystal domain were obtained. Dong and co-workers used a different type of catalyst system with toluene-soluble bis(*tert*-butylphosphine)palladium(0) and water-soluble NaOH as the catalysts to prepare 2D conjugated polymers with carbon–carbon bonds at the interface between toluene and water (Fig. 4b). The reaction was completed in a relatively short time.<sup>47</sup>

### 3.3. On-water surface synthesis

Unlike liquid–liquid interface syntheses, on-water surface synthesis methods can effectively prepare ultra-thin or even single-layer 2D COFs, the Langmuir–Blodgett (LB) method and surfactant-monolayer-assisted interfacial synthesis are the main on-water surface synthesis methods.

Hu and co-workers synthesized a series of single-layer 2D polymers at the air–water interface *via* LB methods (Fig. 5a).<sup>48,49</sup> In the LB method, very small amounts of monomers are needed, and the surface pressure can be precisely controlled. Typically, the monomers were dissolved in a volatile organic solvent such as chloroform or dichloromethane. The LB trough was first filled with deionized water. Then, a mixed solution of monomers was carefully added to the water sub-phase using a micro-

syringe. The volatile organic solvent was allowed to evaporate for 30 min, and then compression was performed at a rate of  $2.98 \text{ mm min}^{-1}$  until the surface pressure reached  $3 \text{ mN m}^{-1}$ . Acetic acid was added to the water sub-phase to initiate the Schiff-base reaction. The reaction was left undisturbed at room temperature. The surface pressure area was recorded by compressing the Teflon barrier. Subsequently, the film was transferred to substrates *via* Langmuir–Blodgett transfer.<sup>48</sup>

In an important breakthrough, in 2019, Feng and co-workers developed the surfactant monolayer-assisted interfacial synthesis (SMAIS) method to guide the preorganization and 2D polycondensation of rigid monomers on the surface of water. Generally, the SMAIS method includes three steps (Fig. 5b): (1) an organized surfactant monolayer is constructed by spreading a molecular surfactant on the water surface to guide the supramolecular arrangement. (2) An aqueous solution of monomer 1 with catalysts is injected to the water. Subsequently, the system is left undisturbed to allow the monomers to diffuse, be absorbed, and pre-organize under the surfactant monolayer. (3) The aqueous solution of monomer 2 with the catalyst is added to initiate 2D interfacial polymerization on the water surface. Importantly, the selection of surfactants was guided by their potential interactions with the monomer precursors, such as electrostatic interactions, hydrogen bonding, coordination bonds and strong covalent bonds. Common surfactants for SMAIS include sodium oleyl sulfate (SOS), stearic acid (SA), sodium dodecyl sulfate (SDS), sodium 4-dodecylbenzenesulfonate (SDBS), and cetyltrimethylammonium bromide (CTAB). In the past five years, Feng and co-workers have successfully synthesized various highly crystalline 2D films, including a 2D polyamide film,<sup>50</sup> quasi-2D polyaniline film,<sup>51</sup> 2D porphyrin-based polyimide film,<sup>52</sup> 2D porphyrin-based polyboronate ester film,<sup>16</sup> 2D porphyrin-based polyimine film,<sup>53</sup> 2D poly(*pyridinium salt*) film,<sup>54</sup> and vinylene-linked 2DPs film.<sup>55</sup>

Rather than a small-molecule surfactant monolayer, Zheng and co-workers used poly(acrylic acid) and poly(sodium 4-styrenesulfonate) (PSS) as polymeric surfactants for SMAIS.<sup>56</sup>

During the synthesis, negatively charged PSS was first spread over the air–water interface, which guided the assembly of the protonated monomers, polymerization and crystallization. For example, a wafer-sized thin film of COF-2,5-Ph was prepared by the Schiff base condensation of 5,10,15,20-tetrakis(4-amino-phenyl)-21*H*,23*H*-porphyrin (TAPP) with 2,5-dihydroxyterephthalaldehyde (2,5-Ph) (Fig. 5c). The thin films achieved an average single-crystalline domain size of around  $3.57 \pm 2.57 \mu\text{m}^2$ .<sup>57</sup> In May 2024, this group published a report in *Nature* detailing a sacrificial go-between guided interfacial synthesis to produce highly strong, tough and elastic 2D single-crystal COF films. Diethylenetriamine served as the go-between, and polyacrylic acid served as the polymeric water surface surfactant for the accumulation and assembly of protonated TAPP through static and hydrogen interactions. 18 h after adding aldehyde monomers to the water, a homogeneous film with large single-crystal domains was obtained, and could be transferred onto arbitrary substrates. The films were connected by an interwoven grain boundary, which endowed them with high strength, toughness and elasticity.<sup>58</sup>



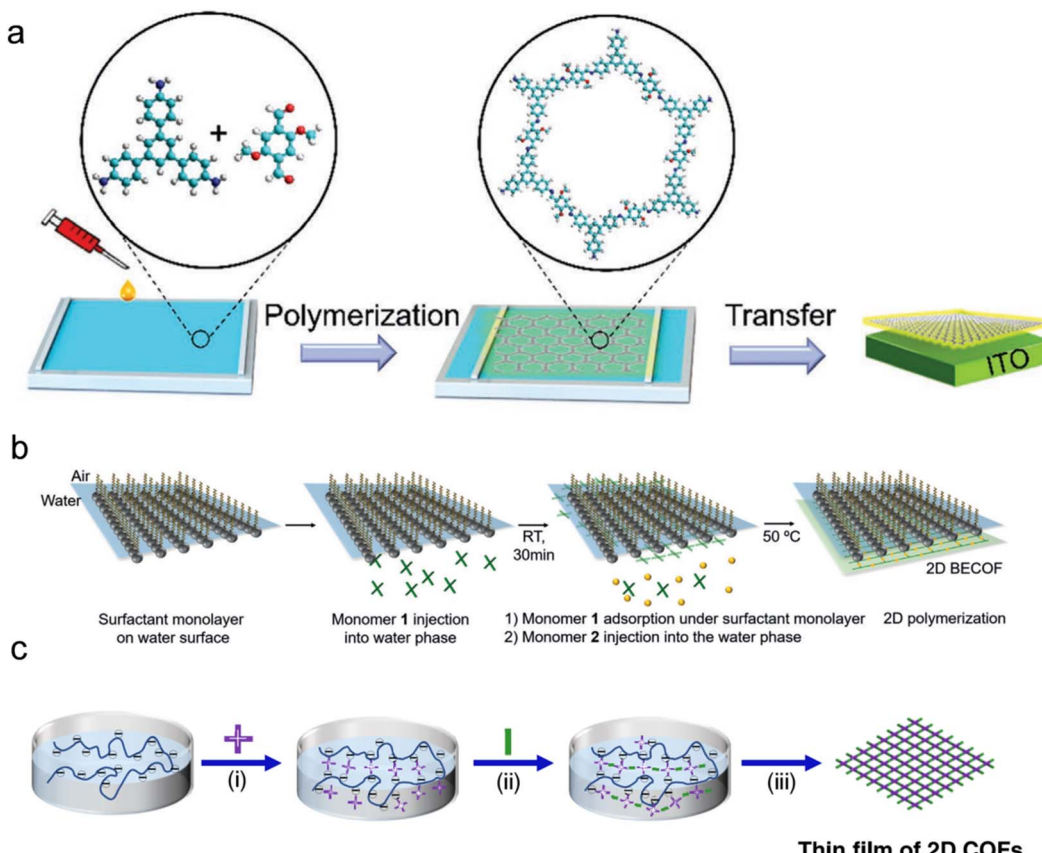


**Fig. 5** (a) Structure and LB synthesis of SL-2DP. Reproduced with permission from ref. 48. Copyright 2023 Wiley-VCH. (b) Synthesis of boronate-ester-linked 2D porphyrin-based COF films via the SMAIS method. Reproduced with permission from ref. 16. Copyright 2020 Wiley-VCH. (c) Schematic of the preparation of 2D COF films through a PSS-mediated on-water surface synthesis. Reproduced with permission from ref. 57. Copyright 2022 American Chemical Society.

### 3.4. Water-phase synthesis

Due to its green and low-cost characteristics, water has recently been considered as a promising reaction medium for synthesizing COFs.<sup>59–61</sup> Common organic monomers have poor solubility in water, which limits the reactions between monomers. Thus, amphiphilic surfactants are used to stabilize the oil–water interface or form a micellar reaction system for synthesizing crystalline COFs. The condensation reaction can be confined on the surfactant-stabilized interface or inside the surfactant nanocompartments.<sup>18,44</sup> In addition, a molecule/water interface was directly created for the synthesis of COFs in water-phase synthesis.

In 2020, Puigmarti-Luis and co-workers developed a biomimetic synthetic method for preparing sub-20 nm imine-based COF aqueous colloidal solutions at room temperature and ambient pressure.<sup>18</sup> As shown in Fig. 6a, the authors employed a catanionic micellar system as reaction nano-compartments; a 97:3 mixture of the cationic surfactant CTAB and anionic surfactant sodium dodecyl sulfate (SDS) was used. In this system, the micellar medium enables the insoluble building blocks (TAPB and BTCA) to be soluble in water at room temperature. The two produced homogeneous solutions of the reactants and acetic acid were mixed to yield the crystalline TAPB–BTCA COF colloids. The reaction mixture was clear and

homogeneous with no apparent precipitation (Fig. 6b). Cryo-TEM of the reaction mixture after 24 h showed two different objects with diameters of  $5 \pm 1$  nm and  $16 \pm 1$  nm (Fig. 6c). In

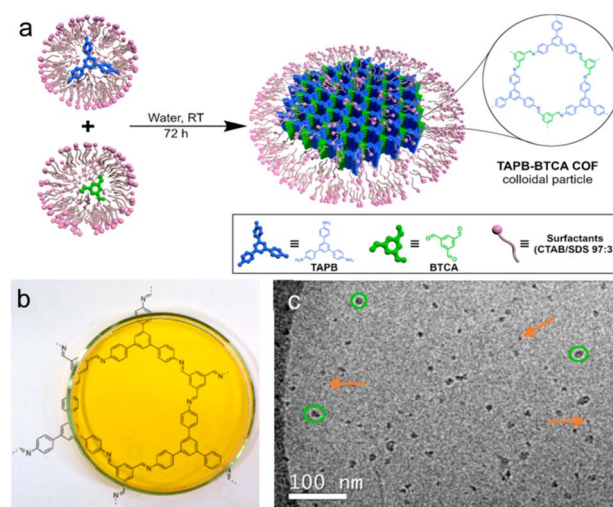


**Fig. 6** (a) The water-phase synthesis of colloidal TAPB–BTCA COF. (b) Photograph of the transparent reaction solution. (c) Cryo-TEM image of TAPB–BTCA COF colloid. Reproduced with permission from ref. 18. Copyright 2020 American Chemical Society.

addition, Wu and co-workers demonstrated a surfactant-free synthesis of C=N-linked COF nanospheres in water at room temperature.<sup>62</sup> A small amount of methyl acetate was adopted as the solvent for TAPB and 2,5-divinylterephthalaldehyde. Then, an aqueous solution of acetic acid was slowly added to the methyl acetate/monomer mixture at a rate of one drop per second. The water-phase system was left undisturbed for 72 h to produce the crystalline COFs. In this surfactant-free synthesis, the formative methyl acetate/water interface, the slow diffusion of the co-solvent and the rapid Schiff base reaction of the monomers together resulted in the nanosphere morphology.

Recently, Xu and co-workers reported a facile, green approach for the synthesis of imine-linked COFs in an aqueous solution at room temperature.<sup>63</sup> The authors achieved the pre-activation of aldehyde monomers using acetic acid to enhance their reactivity in aqueous solutions. As demonstrated by the authors, the aldehyde monomers are not soluble in water, while the 1,4-diaminebenzene (DB) and acetic acid are soluble in water. The insoluble aldehyde monomers reacted with DB along

the created molecule/water interface. In this report, 16 COFs with different molecular structures were successfully synthesized.

### 3.5. Electrosynthesis

Electrochemical technologies, which have the advantages of environmentally friendliness, high efficiency and electric controllability, have been used to develop high-quality organic films.<sup>64</sup> Methods for the electrosynthesis of COFs are divided into two categories: (1) electrophoretic deposition (EPD), which focuses on the directional migration and assembly of charged COF nanoparticles on the electrodes by applying an electric field to their dispersions. (2) Electrosynthesis, in which charged monomers around the electrode surface react directly to form films under an electric field.

In 2019, Medina and co-workers reported EPD techniques for preparing imine- or borate-ester-linked COF films from their COF suspensions (Fig. 7a).<sup>65</sup> Briefly, COF nanoparticle

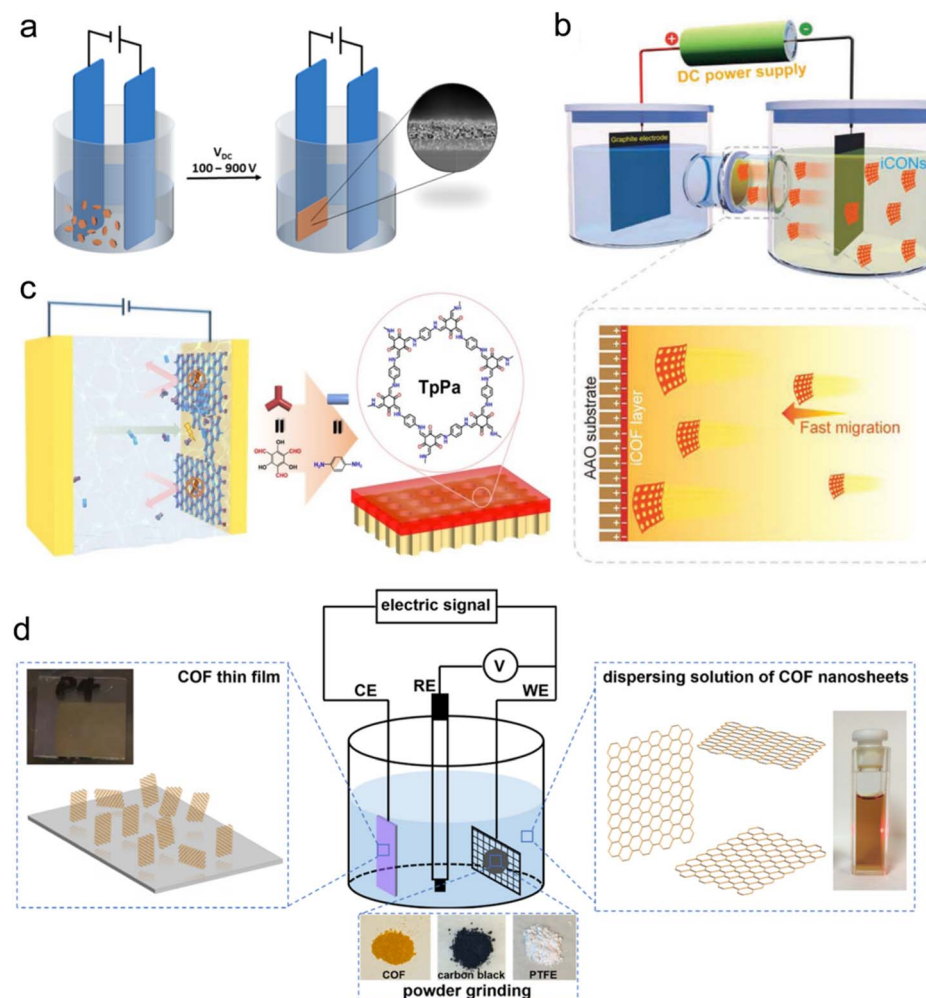


Fig. 7 (a) Schematic of the EPD setup. Reproduced with permission from ref. 65. Copyright 2019 American Chemical Society. (b) Scheme of the fabrication of COF membranes on an AAO substrate via EPD in an H-shaped cell. Reproduced with permission from ref. 66. Copyright 2023 Wiley-VCH. (c) Electrochemical interfacial polymerization of TpPa film on a PAN substrate. Reproduced with permission from ref. 68. Copyright 2023 Wiley-VCH. (d) Electrocleavage synthesis of COF films. Reproduced with permission from ref. 17. Copyright 2019 American Chemical Society.



suspensions were first prepared. Subsequently, electric fields ranging from 100 to 900 V cm<sup>-1</sup> were applied between two electrodes. After 2 min of EPD, 25 cm<sup>2</sup> films were obtained on the electrode surfaces. Wang and co-workers developed a novel two-cell EPD design (Fig. 7b), in which ionic COF nanosheets were assembled into a membrane in the middle of the electric field instead of at the surface of the electrodes.<sup>66</sup> This strategy avoided typical problems including bubbles and acidic/alkaline micro-environments in the near-electrode region. As a result, ultrathin and homogenous COF membranes could be prepared within several minutes.

Wang and co-workers reported a bottom-up electrosynthesis approach to obtain an ionic COF membrane (TpEB).<sup>67</sup> In the system, TpEB films were prepared on ITO under an electric field of 50 V cm<sup>-1</sup>. A brown covering appeared after 3 h of electro-synthesis on the ITO surface. The electrochemical process showed that cationic TpEB nuclei were rapidly formed after mixing of the monomer solutions and migrated to the cathode under the electric field. Subsequently, the dynamic Schiff-base reaction impelled the crystallization of the deposited TpEB nuclei, producing a continuous and smooth film. Very recently, Jiang and co-workers fabricated COF films *via* an electrochemical interfacial polymerization strategy with self-healing and self-inhibiting effects.<sup>68</sup> *N*-Octanoic acid and methanol were chosen as an acid catalyst and reaction solvent (Fig. 7c). The protonated amine monomers and aldehyde monomer migrated to the cathode. Subsequently, through the electrochemical deprotonation reaction and electric field migration of the monomers, the interfacial polymerization was synergistically intensified and the crystallization process was strongly accelerated. The authors demonstrated two inherent effects in the electrochemical process: a self-healing effect for a defect-free morphology and a self-inhibiting effect for an ultrathin film. Based on the above electrochemical results, Qiu and co-workers synthesized electrochromic TPDA-DHBD *via* the Schiff base reaction.<sup>69</sup> The TPDA-DHBD films with redox nature exhibit stable polymorphic colour variations under different applied voltages. Interestingly, Inagi and co-workers reported an *in situ* produced proton source as a Brønsted acid catalyst for the electrosynthesis of C=N bonds, in which the proton sources were produced by the electrochemical oxidation of 1,2-diphenylhydrazine (DPH).<sup>70</sup> The electrogenerated acid from DPH promoted the condensation reaction of amine and aldehyde monomers. The obtained COF films with controlled film thickness showed high crystallinity and porosity. Finally, this synthetic method was also applicable for the synthesis of various imine-based COFs with different 2D or 3D structures. Ma and co-workers developed a combination of electrocleavage and the EPD strategy to prepare imine-linked COF films on electrodes at room temperature (Fig. 7d).<sup>17</sup> Typically, the electrochemical synthesis was performed in a three-electrode electrochemical cell with 0.1 M LiClO<sub>4</sub> in DMF as the electrolyte solution and 0.01 M *p*-toluenesulfonic acid (PTSA) as a proton source. The COF powder was first exfoliated to nanosheets on the cathodic electrode through electrochemical reduction and protonation. Therewith, the exfoliated nanosheets migrated to the anode and underwent anodic oxidation, producing the

Table 1 Key reaction conditions in the electrosynthesis of COFs

Sample	Method	Catalyst	Electrochemical cell	Applied potential	Supporting electrolyte	Reaction time	Ref.
BDT-ETTA COF	EPD	No catalysts	Single-cell system	100 to 900 V cm <sup>-1</sup>	Ethyl acetate	2 min	65
TpPa-SO <sub>3</sub> H	EPD	No catalysts	Two-cell system	20 V cm <sup>-1</sup>	Methanol	2–10 min	66
TpEB	Electrosynthesis	Acetic acid	Single-cell system	50 V cm <sup>-1</sup>	Ethanol	3 h	67
TpPa	Electrosynthesis	<i>n</i> -Octanoic acid	Single-cell system	–7 V	Methanol	4 h	68
TPDA-DHBD	Electrosynthesis	1,2-Diphenylhydrazine	Single-cell system	CV: –0.5 V to 0.5 V vs. Ag/Ag <sup>+</sup>	0.1 M BuNPF <sub>6</sub> in nitromethane	20 cycles	70
TPB-DMTP-COF	Electrocleavage and EPD	0.01 M PTSa	Single-cell system	CV: 0 V to –2 V vs. Ag/Ag <sup>+</sup>	0.1 M LiClO <sub>4</sub> in <i>N,N</i> -dimethylformamide	10 cycles	17



crystalline COF film. For clearer comparison of the effectiveness of the various approaches, the reaction conditions for electro-synthesis are summarized in Table 1.

### 3.6. Sonochemical synthesis

Sonochemical synthesis is an economical and low-power-consumption method.<sup>71,72</sup> The ultrasound synthesis of COFs is driven by acoustic cavitation, in which the formation, growth, and implosive collapse of bubbles occur as ultrasound waves cross through a liquid medium. Ultrasound has also been used to assist solvothermal reactions for controlling crystallization and accelerating gel formation.<sup>73</sup>

In 2012, Ahn and co-workers first reported a sonochemical method for the synthesis of COFs.<sup>74</sup> The crystallization rate in the sonochemical synthesis was accelerated due to the formation and collapse of bubbles in solution, which produces exceedingly high local temperatures and pressures (>1000 bar), resulting in fast heating and cooling rates. COF-1 and COF-5 were synthesized *via* sonochemical synthesis using a 20 kHz, 500 W sonicator for 1 h. The prepared COF-1 exhibited a BET surface area of  $719 \text{ m}^2 \text{ g}^{-1}$ , which was comparable to the reported  $711 \text{ m}^2 \text{ g}^{-1}$  *via* solvothermal synthesis. The BET surface area of COF-5 was  $2122 \text{ m}^2 \text{ g}^{-1}$ , which was significantly higher than the reported  $1590 \text{ m}^2 \text{ g}^{-1}$  for solvothermally prepared COF-5. Cooper and co-workers used a sonochemical synthesis to prepare nine imine-linked COFs in an acidic aqueous medium using a 20 kHz, 550 W sonicator, as shown in Fig. 8.<sup>75</sup> The COFs were successfully synthesized in just 60 min. Their crystallinity and porosity were comparable to or better than those of their counterparts

obtained *via* solvothermal routes. Taking advantage of these simple and efficient methods, the same groups screened 60 crystalline COFs *via* sonochemical synthesis for photocatalytic hydrogen peroxide production using water and oxygen.<sup>76</sup> Simao and co-workers demonstrated that the morphology of the COF films was related to the rate of bubble formation and the maximum bubble size during the ultrasound process.<sup>77</sup>

### 3.7. Single-solution phase synthesis

Single-solution phase synthesis involves monomers that are highly soluble in solvents and can polymerize to a COF at room temperature. Due to the lack of high energy and 2D growth templates, the crystallinity is usually low. To date, all examples prepared by room-temperature homogeneous synthesis are C=N linked COFs without air sensitivity.

In 2021, Wang and co-workers reported meta-structured assemblies of 2D polymers in single-phase solution (dioxane/mesitylene; v/v = 2/3). TAPA-TFPA was synthesized under the catalysis of  $\text{Sc}(\text{OTf})_3$  in the presence of both aniline and benzaldehyde as competitors. Although the reaction finished at room temperature within 1 day, flower-shaped COFs showed high crystallinity.<sup>78</sup> Recently, Jiang and co-workers reported the single solution-phase synthesis of charged COF-NSs with an ultrahigh volume yield of  $18.7 \text{ mg mL}^{-1}$  at room temperature (Fig. 9a). The negatively charged 2,5-diaminobenzenesulfonic acid and 1,3,5-triformylphloroglucinol were selected for polymerization. Dimethyl sulfoxide was selected as the organic solvent. After 24 h at room temperature, the obtained COF showed a spongy solid morphology with aggregated sheets several tens of micrometers

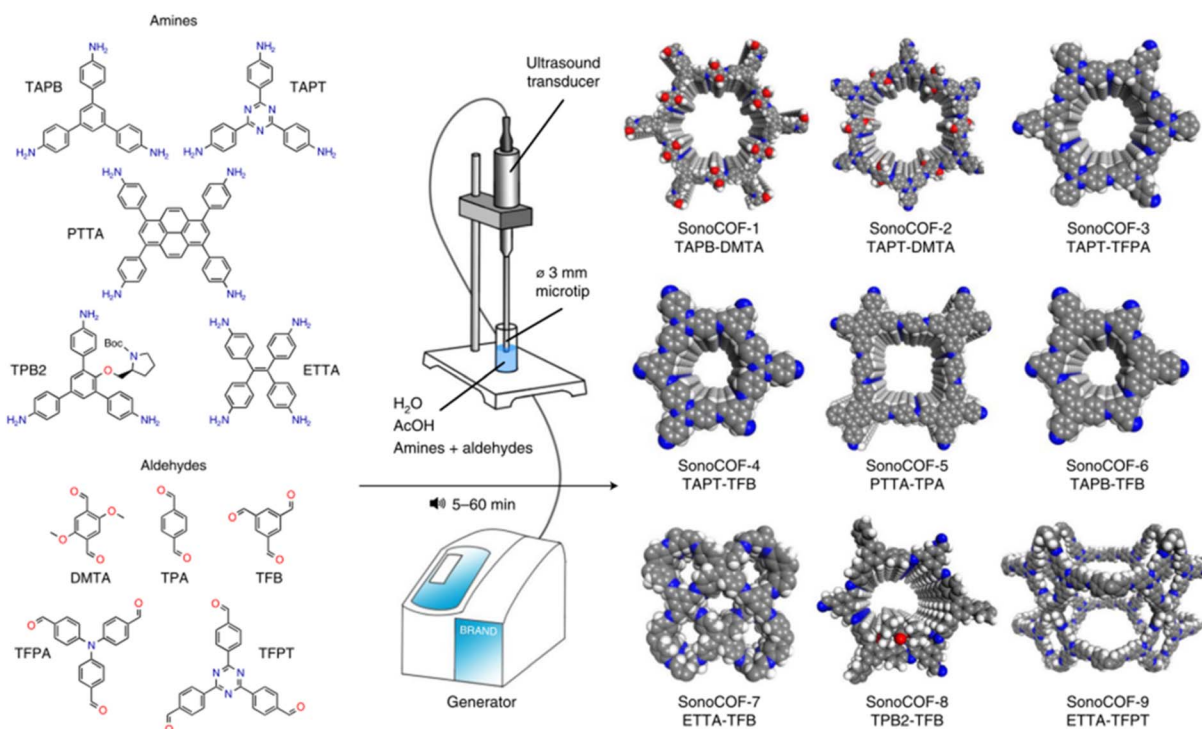


Fig. 8 Sonochemical apparatus and conditions, and COFs synthesized via sonochemical synthesis. Adapted with permission from ref. 73. Copyright 2022 Springer Nature.



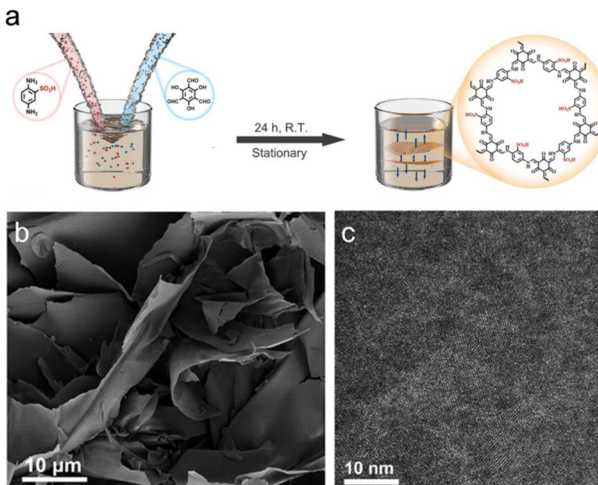


Fig. 9 (a) Room-temperature single solution-phase synthesis process. (b) SEM image. (c) HR-TEM image. Adapted with permission from ref. 79. Copyright 2023 Wiley-VCH.

in width (Fig. 9b). The TEM image exhibited high-order fringes (Fig. 9c). The mechanism of COF-NS growth indicated that charge-induced electrostatic repulsion forces enable in-plane anisotropic secondary growth from initial discrete and disordered polymers into crystalline COF-NSs.<sup>79</sup>

Li and co-workers synthesized the first example of Au-MOFs (JNM-Au-*n*, *n* = 1, 2, 3, 4) *via* the room-temperature Schiff base reaction between cyclic trinuclear gold(i) complexes and aldehyde monomers in mesitylene.<sup>80</sup> Astonishingly, the rapid single-phase synthesis can achieve scalable production (up to 1 g) in 15 min. Very recently, our groups reported the room-temperature single-phase synthesis of semiconducting COFs in DMF.<sup>25</sup> Three COFs were rapidly prepared in 18 h based on the Schiff base reaction between  $C_{3v}$  monomers with tunable planarity and metallized monomers at room temperature. Notably, the room-temperature single-phase synthesis conveniently allowed unprecedented insights into the crystallization mechanism of COFs. A competitive relationship existed between the growth of disordered structures and crystal nuclei. It was found that a twisted structure caused the rapid formation of amorphous structures and a slow dynamic crystallization rate, while highly planar monomers boosted the formation and the rapid growth of crystal nuclei. Very recently, Dong and co-workers reported the first example of  $\beta$ -ketoamine-linked COFs *via* room temperature Mannich reaction, in which a mixture of methanol (2.6 mL) and acetonitrile (1.3 mL) was used as the reaction solvent and  $\text{CeCl}_3$  served as the catalyst.<sup>81</sup> After 7 days of the condensation polymerization of 4,4',4''-(1,3,5-triazine-2,4,6-triyl)tribenzaldehyde, acetophenone, and 4,4'-diaminodiphenyl, red TAD-COF solids were successfully prepared in 75.1% yield.

### 3.8. Mechanochemical synthesis

Mechanochemical reactions are induced by the direct absorption of mechanical energy. In mechanochemical synthesis, the

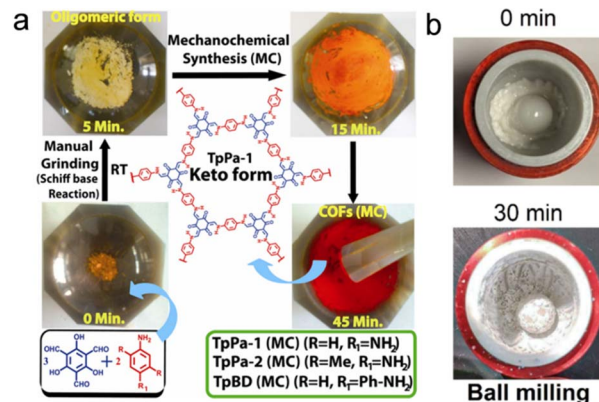


Fig. 10 (a) Scheme of the mechanochemical synthesis of TpPa-1, TpPa-2, and TpBD through simple grinding using a mortar and pestle. Reproduced with permission from ref. 82. Copyright 2013 American Chemical Society. (b) Photographs of the reaction mixture for the synthesis of COF-1 before and after ball-milling. Adapted with permission from ref. 26. Copyright 2024 Wiley-VCH.

chemical bonds are formed during the grinding of solid reactants in a mortar or ball mill.

Banerjee and co-workers reported the first solvent-free room-temperature mechanochemical synthesis of three  $\beta$ -ketoamine-linked COFs (TpPa-1, TpPa-2, and TpBD) using a mortar and pestle (Fig. 10a).<sup>82</sup> The grinding reaction time was only 40 min. XRD analysis of the  $\beta$ -ketoamine-linked COFs showed high crystallinity. Unsatisfactorily, three COFs exhibited small BET surface areas of  $61 \text{ m}^2 \text{ g}^{-1}$  for TpPa-1,  $56 \text{ m}^2 \text{ g}^{-1}$  for TpPa-2, and  $35 \text{ m}^2 \text{ g}^{-1}$  for TpBD, which were lower than those of the corresponding products obtained *via* solvothermal synthesis.

Furthermore, this group investigated liquid-assisted grinding (LAG) *via* adding a few drops of organic solvent and aqueous acid catalyst to the monomer mixture.<sup>83</sup> A new crystalline hydrazone-linked COF (TpTh) and reported materials such as DhaTph and Lzu-1 were successfully prepared by applying the LAG approach. Similarly, Sukumaran and co-workers synthesized 1 kg of Tp-Azo *via* the LAG approach with a planetary mixer.<sup>84</sup> Cheetham and coworkers reported a cocrystal precursor template strategy *via* liquid-assisted mechanochemical synthesis in a ball mill.<sup>27</sup> Benefiting from the cocrystal precursor, interlayer hydrogen bonding between the amine and PTSA created a cocrystal template for the condensation reaction with aldehydes, and then the aldehydes reacted *via* confined polymerization from the cocrystal synthons to COFs. Very recently, Perepichka and co-workers reported the first mechanochemical synthesis of boroxine-linked COF-1 (ref. 26) and the first example of a mechanochemically prepared 3D COF (COF-102). Using trimethyl-boroxine as a dehydrating additive, the hydrolytic sensitivity of the boroxine-based COFs was overcome. The resulting COFs showed high crystallinity and porosity. As shown in Fig. 10b, COF-1 can be synthesized rapidly *via* ball-milling. By using resonant acoustic mixing (RAM), which enabled direct input of mechanical energy to the samples, COF-1 was readily scaled up to 10 grams.



### 3.9. High-energy ionizing radiation synthesis

Due to their ionization of the entire reaction system, high-energy ionizing radiation sources such as  $\gamma$  rays and electron beams have been utilized to produce extremely reactive species, which enable the reagents to directly gain energy to bypass the activation barrier of the reaction and hasten the reaction process.

In 2020, Wang and co-workers reported the radiation-induced synthesis of 2D imine COFs *via* a high energy electron beam (Fig. 11a).<sup>85</sup> Typically, COF precursors and an aqueous acetic acid catalyst were sealed under a nitrogen atmosphere. The system was irradiated by the electron beam for 160 s with a cumulative absorbed dose of 100 kGy. As the electron beam dose was increased, it was found that lower doses produced poor crystallinity, while higher doses resulted in structural degradation of the COFs. In addition, first-principles calculations demonstrated that the free radicals (*e.g.* H $^{\cdot}$ , OH $^{\cdot}$ , and R-NH $^{\cdot}$ ) formed under irradiation can activate the intermediate and lower the reaction barrier. The same groups synthesized polymer-grafted COFs *in situ* *via* a simple  $^{60}$ Co  $\gamma$ -ray irradiated one-pot reaction under ambient conditions, in which the Schiff base reaction and free radical polymerization can occur simultaneously.<sup>86</sup> In addition, Chou and co-workers adopted gamma irradiation to synthesize imine-linked and imide-linked COFs at room temperature under open-air

conditions within 1 h (Fig. 11b).<sup>87</sup> As shown in Fig. 11c, with increased  $\gamma$ -ray intensity, the resulting COF showed increased crystallinity. In addition, compared with their counterparts synthesized *via* the solvothermal method, the COFs obtained *via* gamma irradiation showed improved crystallinity, surface area, and thermal stability.

### 3.10. Photochemical synthesis

Photochemical synthesis involves the fact that under the illumination of light, organic molecules or groups can be activated to form new linkages compared with their counterparts in the ground state.<sup>88</sup> Among the photochemical reactions, in terms of energy- and resource-saving requirements, “window ledge” reactions that can be directly activated by natural sunlight are important candidate reactions to prepare COFs.<sup>89</sup> In addition, some highly-efficient photocatalytic reactions catalyzed under artificial light sources can also be used to synthesize COFs.<sup>90</sup> The light intensity and light wavelength depend on the selected reaction type.

In 2022, Dong and co-workers first reported the sunlight-driven photocatalytic synthesis of a benzoxazole-linked COF (LZU-191) under ambient conditions (Fig. 12a).<sup>89</sup> The photocatalytic cyclization reaction of 2,5-diamino-1,4-benzenediol dihydrochloride and 1,3,5-tris(4-formylphenyl)triazine in oxygen was conducted in dimethylacetamide using *N*-methyl-2-pyrrolidone as a base and TBA-eosin Y as a visible-light photocatalyst. Benzoxazole-linked LZU-191 was obtained as a deep

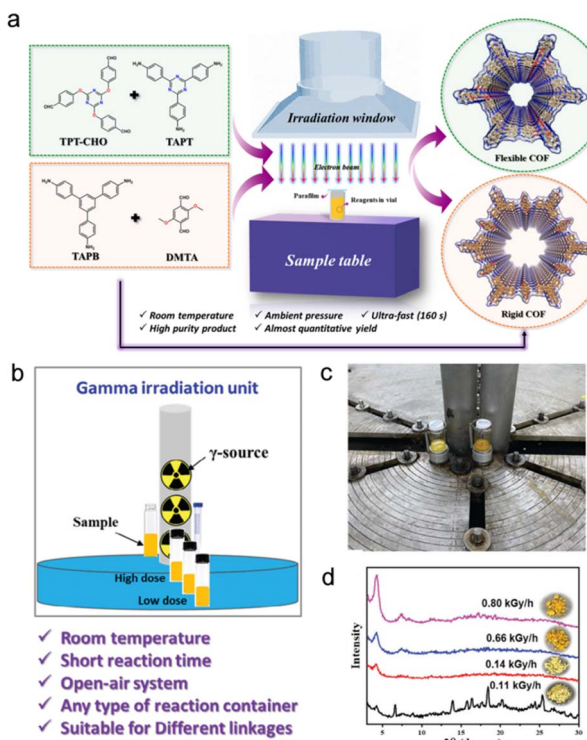


Fig. 11 (a) Experimental setup of the electron beam accelerator and the synthesized crystalline COFs. Reproduced with permission from ref. 85. Copyright 2020 American Chemical Society. (b) Illustration of the gamma irradiation unit. (c) The synthetic set-up. (d) XRD patterns of products obtained under different  $\gamma$ -ray intensities. Adapted with permission from ref. 87. Copyright 2024 Wiley-VCH.

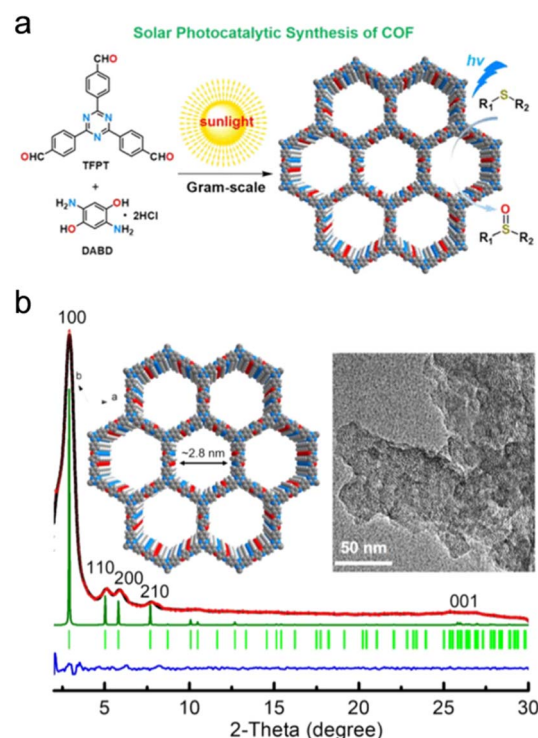


Fig. 12 (a) Photochemical synthesis of LZU-191 under natural sunlight. (b) PXRD patterns of LZU-191; top inset: crystal structure and TEM image of LZU-191. Reproduced with permission from ref. 89. Copyright 2022 American Chemical Society.



Table 2 Main parameters for the room-temperature synthesis of representative COFs

Sample	Method	Room-temperature conditions	Yield	BET surface area	Crystallinity	State	Ref.
COF-DT	Solid-liquid interfacial synthesis	48 h	Not available	Not available	High crystallinity	COF film	37
Tp-Bpy	Liquid-liquid interfacial synthesis	72 h	23%	1151 m <sup>2</sup> g <sup>-1</sup>	High crystallinity	COF film	31
2DP	LB method	12 h	Not available	Not available	High crystallinity	COF film	48
2D COF-1 film	On-water surface synthesis	18 h	Not available	Not available	High crystallinity	COF film	58
TAPB-BTCA COF	Water-phase synthesis	72 h	88%	687 m <sup>2</sup> g <sup>-1</sup>	High crystallinity	COF colloid	18
TpEB	Electrosynthesis	3 h	Not available	239.3 m <sup>2</sup> g <sup>-1</sup>	High crystallinity	COF film	67
COF-1; COF-5	Sonochemical synthesis	20 kHz, 500 W sonicator, 1 h	100% (COF-1); 50% (COF-5)	719 m <sup>2</sup> g <sup>-1</sup> ; 2122 m <sup>2</sup> g <sup>-1</sup>	High crystallinity; high crystallinity	COF powder	61
JNM-Au-1	Single-solution phase synthesis	15 min	99%	351.01 m <sup>2</sup> g <sup>-1</sup>	High crystallinity	COF powder	74
Tp-PPa-1	Mechanochemical synthesis	Mortar and pestle, 40 min	90%	61 m <sup>2</sup> g <sup>-1</sup>	High crystallinity	COF powder	82
EB-COF-1	High-energy ionizing radiation synthesis	Electron beam irradiation, 160 s	92%	738 m <sup>2</sup> g <sup>-1</sup>	High crystallinity	COF powder	85
LZU-191	Photochemical synthesis	Natural sunlight, 48 h	73% (1.21 g)	1314 m <sup>2</sup> g <sup>-1</sup>	High crystallinity	COF powder	89

yellow solid under natural sunlight irradiation for 48 h, exhibited high crystallinity with an intense (100) plane peak at 2.92° (Fig. 12b), and could effectively drive the visible-light-catalytic aerobic oxidation of sulfides to sulfoxides. Recently, this group also reported a photoredox-catalyzed multicomponent Petasis reaction for the synthesis of COFs under ambient conditions, in which aromatic aldehydes, amines, and potassium cyclo-hexyltrifluoroborate in the presence of  $[\text{Ir}(\text{dtbbpy})(\text{ppy})_2]\text{PF}_6$  produced crystalline COFs at room temperature.<sup>90</sup> Upon visible-light irradiation for 72 h, a series of COFs, including Cy-N3-COF, Cy-LZU-1, Cy-COF-42, and TPB-DMTP-COF, were successfully synthesized with excellent crystallinity and stability. In addition, photochemically induced cycloaddition reactions including [4 + 4]-cycloadditions of anthracenes and [2 + 2]-cycloadditions of olefins can be used to obtain COFs that show smart response behavior.<sup>91–94</sup> Recently, Lim and coworkers presented a novel approach for synthesizing 2D COF thin films by combining photochemistry and a liquid flow system.<sup>95</sup> The photochemical approach can offer spatially controllable energy sources for patternable COF films. Finally, an ultrasmooth patterned high-crystalline 2D COF film on hexagonal boron nitride was successfully fabricated.

Novel room-temperature synthetic strategies have been classified based on their use of green solvents, confined interfaces, assisted energy sources and crystallization factors (Table 2). Despite the obvious progress that has been made in the room-temperature synthesis of COFs, there is still a long way to go before its industrialization.

## 4. Conclusions and perspectives

In this review, we have presented and discussed advanced characterization technologies and the emerging room-temperature synthetic techniques for the preparation of COF powders or COF films. A variety of synthetic methods have facilitated the rapid and green synthesis of COFs. Compared with high-temperature solvothermal synthesis, room-temperature synthesis is more eco-friendly and has lower energy consumption. The development of room-temperature synthesis will promote the large-scale and green preparation of COFs.

(1) Due to the rapid synthesis and non-oriented growth, most synthesized COFs are still polycrystalline. Some C=N-linked COF single crystals have been synthesized. However, the development of a variety of COF single crystals is highly desirable but challenging. More efforts should be devoted to determining how to control the experimental conditions to promote single-crystal domains.

(2) The reactions that can be utilized for the room-temperature synthesis of COFs are limited. Thus, the development and design of more reactions for the room-temperature synthesis of COFs are highly desirable. Constructing more room temperature reactions would not only greatly broaden the diversity of COF structures but also enrich their chemistry and physics. Various reversible or irreversible reactions should be further explored for the room-temperature synthesis of COF powders and COF films.



(3) Controlling and revealing the framework growth process are interesting and very important for highly efficient room temperature synthesis. The crystallization mechanism will vary depending on the selected type of monomers, catalyst, reaction system, reaction type, the solubility of the monomers, *etc.* Thus, monitoring the crystallization process in detail *via* advanced *in situ* characterization technologies will drive the rapid development and application of COFs.

(4) Compared with those achieved *via* solvothermal synthesis, the diversity of COF structures and the topological design of COFs *via* room-temperature synthesis are still lacking. Thus, focusing on the design of chemical structures and topological structures is clearly important for exploring potential applications.

(5) In room-temperature synthesis, there are two challenges: (1) a longer reaction time may be needed due to the slower reaction rate; (2) a low reaction temperature may not meet the activation energy requirements for novel condensation reactions. Thus, key assistance technologies must be developed to accelerate room-temperature synthesis. In future, exploring novel approaches to highly crystalline COFs using eco-friendly solvents and low-energy assistance methods will be more attractive. Faster and more-efficient synthesis are becoming the research focus in the COF field.

## Data availability

Data available on request from the authors. The data that support the findings of this study are available from the corresponding author upon reasonable request.

## Author contributions

D. Wu designed the structure of the review and wrote the original draft. N. Gu, J. Yao, Y. Cao, L. Wang, I. Shakir collected the papers for this review topic. Y. Xu and Y. Sun supervised the review and revised the manuscript. Finally, the manuscript was revised by all authors.

## Conflicts of interest

The authors declare no conflict of interest.

## Acknowledgements

The authors acknowledge the financial supports from National Natural Science Foundation of China (52473221, 22022510), Shanxi Provincial Natural Science Foundation (202403021212051, TZLH20230818009, 202204021301049, 202304021301030 YDZJSX20231A060, 2024030212121), Scientific and Technological Innovation Programs of Higher Education Institutions in Shanxi (2024L166). I. S. acknowledges a research grant funded by the Research, Development, and Innovation Authority (RDIA) – Kingdom of Saudi Arabia – with grant number (12615-iu-2023-IU-R-2-1-EI-).

## Notes and references

- K. Geng, T. He, R. Liu, S. Dalapati, K. T. Tan, Z. Li, S. Tao, Y. Gong, Q. Jiang and D. Jiang, Covalent Organic Frameworks: Design, Synthesis, and Functions, *Chem. Rev.*, 2020, **120**, 8814–8933.
- M. E. Belowich and J. F. Stoddart, Dynamic imine chemistry, *Chem. Soc. Rev.*, 2012, **41**, 2003–2024.
- S. Xu, M. Richter and X. Feng, Vinylene-Linked Two-Dimensional Covalent Organic Frameworks: Synthesis and Functions, *Acc. Mater. Res.*, 2021, **2**, 252–265.
- Y. Liu, S. Fu, D. L. Pastoetter, A. H. Khan, Y. Zhang, A. Dianat, S. Xu, Z. Liao, M. Richter, M. Yu, M. Položij, E. Brunner, G. Cuniberti, T. Heine, M. Bonn, H. I. Wang and X. Feng, Vinylene-Linked 2D Conjugated Covalent Organic Frameworks by Wittig Reactions, *Angew. Chem., Int. Ed.*, 2022, **61**, e202209762.
- F. Meng, S. Bi, Z. Sun, D. Wu and F. Zhang, 2,4,6-Trimethylpyridine-Derived Vinylene-Linked Covalent Organic Frameworks for Confined Catalytic Esterification, *Angew. Chem., Int. Ed.*, 2022, **61**, e202210447.
- S. Bi, F. Meng, D. Wu and F. Zhang, Synthesis of Vinylene-Linked Covalent Organic Frameworks by Monomer Self-Catalyzed Activation of Knoevenagel Condensation, *J. Am. Chem. Soc.*, 2022, **144**, 3653–3659.
- L. Liu, Y. Gong, Y. Tong, H. Tian, X. Wang, Y. Hu, S. Huang, W. Huang, S. Sharma, J. Cui, Y. Jin, W. Gong and W. Zhang, Imidazole-Linked Fully Conjugated Covalent Organic Framework for High-Performance Sodium-Ion Battery, *CCS Chem.*, 2024, **6**, 1255–1263.
- N. Arora, C. Flores, C. Senarathna Milinda, M. Thompson Christina and A. Smaldone Ronald, Design, Synthesis, and Applications of Mesoporous Covalent Organic Frameworks, *CCS Chem.*, 2023, **6**, 57–68.
- M. Zhang, M. Lu, M.-Y. Yang, J.-P. Liao, Y.-F. Liu, H.-J. Yan, J.-N. Chang, T.-Y. Yu, S.-L. Li and Y.-Q. Lan, Ultrafine Cu nanoclusters confined within covalent organic frameworks for efficient electroreduction of CO<sub>2</sub> to CH<sub>4</sub> by synergistic strategy, *eScience*, 2023, **3**, 100116.
- Y. Liu, S. Fu, D. L. Pastoetter, A. H. Khan, Y. Zhang, A. Dianat, S. Xu, Z. Liao, M. Richter, M. Yu, M. Položij, E. Brunner, G. Cuniberti, T. Heine, M. Bonn, H. I. Wang and X. Feng, Vinylene-Linked 2D Conjugated Covalent Organic Frameworks by Wittig Reactions, *Angew. Chem., Int. Ed.*, 2022, **61**, e202209762.
- K. Mou, F. Meng, Z. Zhang, X. Li, M. Li, Y. Jiao, Z. Wang, X. Bai and F. Zhang, Pyridazine-Promoted Construction of Vinylene-Linked Covalent Organic Frameworks with Exceptional Capability of Stepwise Water Harvesting, *Angew. Chem., Int. Ed.*, 2024, **63**, e202402446.
- B. Feng, X. Chen, P. Yan, S. Huang, C. Lu, H. Ji, J. Zhu, Z. Yang, K. Cao and X. Zhuang, Isomeric Dual-Pore Two-Dimensional Covalent Organic Frameworks, *J. Am. Chem. Soc.*, 2023, **145**, 26871–26882.
- G. Fu, D. Yang, S. Xu, S. Li, Y. Zhao, H. Yang, D. Wu, P. S. Petkov, Z.-A. Lan, X. Wang and T. Zhang,



Construction of Thiadiazole-Bridged  $sp^2$ -Carbon-Conjugated Covalent Organic Frameworks with Diminished Excitation Binding Energy Toward Superior Photocatalysis, *J. Am. Chem. Soc.*, 2024, **146**, 1318–1325.

14 S. Yuan, X. Li, J. Zhu, G. Zhang, P. Van Puyvelde and B. Van der Bruggen, Covalent organic frameworks for membrane separation, *Chem. Soc. Rev.*, 2019, **48**, 2665–2681.

15 H. Wang, Z. Zeng, P. Xu, L. Li, G. Zeng, R. Xiao, Z. Tang, D. Huang, L. Tang, C. Lai, D. Jiang, Y. Liu, H. Yi, L. Qin, S. Ye, X. Ren and W. Tang, Recent progress in covalent organic framework thin films: fabrications, applications and perspectives, *Chem. Soc. Rev.*, 2019, **48**, 488–516.

16 S. Park, Z. Liao, B. Ibarlucea, H. Qi, H.-H. Lin, D. Becker, J. Melidonie, T. Zhang, H. Sahabudeen, L. Baraban, C.-K. Baek, Z. Zheng, E. Zschech, A. Fery, T. Heine, U. Kaiser, G. Cuniberti, R. Dong and X. Feng, Two-Dimensional Boronate Ester Covalent Organic Framework Thin Films with Large Single Crystalline Domains for a Neuromorphic Memory Device, *Angew. Chem., Int. Ed.*, 2020, **59**, 8218–8224.

17 L. Wang, C. Xu, W. Zhang, Q. Zhang, M. Zhao, C. Zeng, Q. Jiang, C. Gu and Y. Ma, Electrocleavage Synthesis of Solution-Processed, Imine-Linked, and Crystalline Covalent Organic Framework Thin Films, *J. Am. Chem. Soc.*, 2022, **144**, 8961–8968.

18 C. Franco, D. Rodríguez-San-Miguel, A. Sorrenti, S. Sevim, R. Pons, A. E. Platero-Prats, M. Pavlovic, I. Szilágyi, M. L. Ruiz Gonzalez, J. M. González-Calbet, D. Bochicchio, L. Pesce, G. M. Pavan, I. Imaz, M. Cano-Sarabia, D. Maspoch, S. Pané, A. J. de Mello, F. Zamora and J. Puigmartí-Luis, Biomimetic Synthesis of Sub-20 nm Covalent Organic Frameworks in Water, *J. Am. Chem. Soc.*, 2020, **142**, 3540–3547.

19 S. Liu, L. Wei, T. Zeng, W. Jiang, Y. Qiu, X. Yao, Q. Wang, Y. Zhao and Y.-B. Zhang, Single-Crystal Dynamic Covalent Organic Frameworks for Adaptive Guest Alignments, *J. Am. Chem. Soc.*, 2024, **146**, 34053–34063.

20 S. Wang, V. A. Reddy, M. C.-Y. Ang, J. Cui, D. T. Khong, Y. Han, S. I. Loh, R. Cheerlavancha, G. P. Singh, S. Rajani and M. S. Strano, Single-Crystal 2D Covalent Organic Frameworks for Plant Biotechnology, *J. Am. Chem. Soc.*, 2023, **145**, 12155–12163.

21 J. Han, J. Feng, J. Kang, J.-M. Chen, X.-Y. Du, S.-Y. Ding, L. Liang and W. Wang, Fast growth of single-crystal covalent organic frameworks for laboratory X-ray diffraction, *Science*, 2024, **383**, 1014–1019.

22 H. Lv, X. Zhu, J. Mei, Y. Xia and B. Wang, Recent progress of *in situ* characterization of  $\text{LiNi}_{1-x-y}\text{Co}_x\text{Mn}_y\text{O}_2$  cathodes for lithium metal batteries: a mini review, *Nano Res.*, 2024, **17**, 1384–1401.

23 H. S. Sasmal, A. Halder, S. Kunjattu H, K. Dey, A. Nadol, T. G. Ajithkumar, P. Ravindra Bedadur and R. Banerjee, Covalent Self-Assembly in Two Dimensions: Connecting Covalent Organic Framework Nanospheres into Crystalline and Porous Thin Films, *J. Am. Chem. Soc.*, 2019, **141**, 20371–20379.

24 X.-M. Lin, Y.-L. Sun, Y.-X. Chen, S.-X. Li and J.-F. Li, Insights into electrocatalysis through *in situ* electrochemical surface-enhanced Raman spectroscopy, *eScience*, 2024, 100352, DOI: [10.1016/j.esci.2024.100352](https://doi.org/10.1016/j.esci.2024.100352).

25 D. Wu, Q. Zhang, S. Yin, C. Song, N. Gu, D. Wang, T. Cai and B. Zhang, Room-Temperature Single-Phase Synthesis of Semiconducting Metal-Covalent Organic Frameworks With Microenvironment-Tuned Photocatalytic Efficiency, *Small Methods*, 2024, 2401284, DOI: [10.1002/smtd.202401284](https://doi.org/10.1002/smtd.202401284).

26 E. Hamzehpoor, F. Effaty, T. H. Borchers, R. S. Stein, A. Wahrhaftig-Lewis, X. Ottenwaelder, T. Friščić and D. F. Perepichka, Mechanochemical Synthesis of Boroxine-linked Covalent Organic Frameworks, *Angew. Chem., Int. Ed.*, 2024, **63**, e202404539.

27 H. Chen, D. Feng, F. Wei, F. Guo and A. K. Cheetham, Hydrogen-bond-regulated mechanochemical synthesis of covalent organic frameworks: cocrystal precursor strategy for confined assembly, *Angew. Chem., Int. Ed.*, 2024, e202415454, DOI: [10.1002/anie.202415454](https://doi.org/10.1002/anie.202415454).

28 S. T. Emmerling, L. S. Germann, P. A. Julien, I. Moudrakovski, M. Etter, T. Friščić, R. E. Dinnebier and B. V. Lotsch, *In situ* monitoring of mechanochemical covalent organic framework formation reveals templating effect of liquid additive, *Chem.*, 2021, **7**, 1639–1652.

29 Y. Wen, S. Ding, C. Ma, P. Jia, W. Tu, Y. Guo, S. Guo, W. Zhou, X. Zhang, J. Huang, L. Zhang, T. Shen and Y. Qiao, *In situ* TEM visualization of Ag catalysis in  $\text{Li-O}_2$  nanobatteries, *Nano Res.*, 2023, **16**, 6833–6839.

30 D. Wu, Q. Zhang, X. Wang and B. Zhang, Interface-confined synthesis of a nonplanar redox-active covalent organic framework film for synaptic memristors, *Nanoscale*, 2023, **15**, 2726–2733.

31 K. Dey, M. Pal, K. C. Rout, S. Kunjattu H, A. Das, R. Mukherjee, U. K. Kharul and R. Banerjee, Selective Molecular Separation by Interfacially Crystallized Covalent Organic Framework Thin Films, *J. Am. Chem. Soc.*, 2017, **139**, 13083–13091.

32 Q. Zheng, A. Ren, A. Zagalskaya, H. Mao, D. Lee, C. Yang, K. C. Bustillo, L. F. Wan, T. A. Pham, J. A. Reimer, J. Zhang, Y. Liu and H. Zheng, Multistep Growth Pathway of Covalent Organic Framework Onion Nanostructures, *J. Am. Chem. Soc.*, 2024, **146**, 34167–34175.

33 C. Yang, K. Jiang, Q. Zheng, X. Li, H. Mao, W. Zhong, C. Chen, B. Sun, H. Zheng, X. Zhuang, J. A. Reimer, Y. Liu and J. Zhang, Chemically Stable Polyarylether-Based Metallophthalocyanine Frameworks with High Carrier Mobilities for Capacitive Energy Storage, *J. Am. Chem. Soc.*, 2021, **143**, 17701–17707.

34 Y. He and X. Lin, Fabricating compact covalent organic framework membranes with superior performance in dye separation, *J. Membr. Sci.*, 2021, **637**, 119667.

35 L. Cao, X. Liu, D. B. Shinde, C. Chen, I. C. Chen, Z. Li, Z. Zhou, Z. Yang, Y. Han and Z. Lai, Oriented Two-Dimensional Covalent Organic Framework Membranes with High Ion Flux and Smart Gating Nanofluidic Transport, *Angew. Chem., Int. Ed.*, 2022, **61**, e202113141.



36 D. D. Medina, J. M. Rotter, Y. Hu, M. Dogru, V. Werner, F. Auras, J. T. Markiewicz, P. Knochel and T. Bein, Solid-Liquid Interfacial Engineered Large-Area Two-Dimensional Covalent Organic Framework Films, *J. Am. Chem. Soc.*, 2015, **137**, 1016–1019.

37 L. Cao, X. Liu, D. B. Shinde, C. Chen, I. C. Chen, Z. Li, Z. Zhou, Z. Yang, Y. Han and Z. Lai, Oriented Two-Dimensional Covalent Organic Framework Membranes with High Ion Flux and Smart Gating Nanofluidic Transport, *Angew. Chem., Int. Ed.*, 2022, **61**, e202113141.

38 J. Hong, M. Liu, Y. Liu, S. Shang, X. Wang, C. Du, W. Gao, C. Hua, H. Xu, Z. You, Y. Liu and J. Chen, Solid-Liquid Interfacial Engineered Large-Area Two-Dimensional Covalent Organic Framework Films, *Angew. Chem., Int. Ed.*, 2024, **63**, e202317876.

39 A. Kumar Mahato, S. Bag, H. S. Sasmal, K. Dey, I. Giri, M. Linares-Moreau, C. Carbonell, P. Falcaro, E. B. Gowd, R. K. Vijayaraghavan and R. Banerjee, Crystallizing Sub 10 nm Covalent Organic Framework Thin Films via Interfacial-Residual Concomitance, *J. Am. Chem. Soc.*, 2021, **143**, 20916–20926.

40 M. K. Hota, S. Chandra, Y. Lei, X. Xu, M. N. Hedhili, A.-H. Emwas, O. Shekhah, M. Eddaoudi and H. N. Alshareef, Electrochemical Thin-Film Transistors using Covalent Organic Framework Channel, *Adv. Funct. Mater.*, 2022, **32**, 2201120.

41 S. Gao, Z. Li, Y. Yang, Z. Wang, Y. Wang, S. Luo, K. Yao, J. Qiu, H. Wang, L. Cao, Z. Lai and J. Wang, The Ionic Liquid-H<sub>2</sub>O Interface: A New Platform for the Synthesis of Highly Crystalline and Molecular Sieving Covalent Organic Framework Membranes, *ACS Appl. Mater. Interfaces*, 2021, **13**, 36507–36516.

42 D. Yadav, A. Kumar, J. Y. Kim, N.-J. Park and J.-O. Baeg, Interfacially synthesized 2D COF thin film photocatalyst: efficient photocatalyst for solar formic acid production from CO<sub>2</sub> and fine chemical synthesis, *J. Mater. Chem. A*, 2021, **9**, 9573–9580.

43 M. Matsumoto, L. Valentino, G. M. Stiehl, H. B. Balch, A. R. Corcos, F. Wang, D. C. Ralph, B. J. Mariñas and W. R. Dichtel, Lewis-Acid-Catalyzed Interfacial Polymerization of Covalent Organic Framework Films, *Chem*, 2018, **4**, 308–317.

44 Y. Ma, S. Yu, W. Li, D. Chen, Z. Zheng, L. Mao, X. Yang, W.-J. Wang and P. Liu, Rapid yet Controlled Synthesis of 2D Covalent Organic Framework Nanocapsules as High-Performance Photocatalytic Carriers, *Angew. Chem., Int. Ed.*, 2024, e202416980, DOI: [10.1002/anie.202416980](https://doi.org/10.1002/anie.202416980).

45 D. Zhou, X. Tan, H. Wu, L. Tian and M. Li, Synthesis of C–C Bonded Two-Dimensional Conjugated Covalent Organic Framework Films by Suzuki Polymerization on a Liquid-Liquid Interface, *Angew. Chem., Int. Ed.*, 2019, **58**, 1376–1381.

46 D. Wu, Q. Che, H. He, M. E. El-Khouly, S. Huang, X. Zhuang, B. Zhang and Y. Chen, Room-Temperature Interfacial Synthesis of Vinylene-Bridged Two-Dimensional Covalent Organic Framework Thin Film for Nonvolatile Memory, *ACS Mater. Lett.*, 2023, **5**, 874–883.

47 Y. Li, Y. Wang, Y. Zou, X. Zhang, H. Dong and W. Hu, Two-Dimensional Conjugated Polymer Synthesized by Interfacial Suzuki Reaction: Towards Electronic Device Applications, *Angew. Chem., Int. Ed.*, 2020, **59**, 9403–9407.

48 L. Liu, B. Geng, W. Ji, L. Wu, S. Lei and W. Hu, A Highly Crystalline Single Layer 2D Polymer for Low Variability and Excellent Scalability Molecular Memristors, *Adv. Mater.*, 2023, **35**, 2208377.

49 L. Liu, W. Ji, W. He, Y. Cheng, R. Hao, P. Hao, H. Dong, X. Ding, S. Lei, B. Han and W. Hu, Rational Design of Fluorinated 2D Polymer Film Based on Donor-Acceptor Architecture toward Multilevel Memory Device for Neuromorphic Computing, *Adv. Mater.*, 2024, **36**, 2405328.

50 K. Liu, H. Qi, R. Dong, R. Shivhare, M. Addicoat, T. Zhang, H. Sahabudeen, T. Heine, S. Mannsfeld, U. Kaiser, Z. Zheng and X. Feng, On-water surface synthesis of crystalline, few-layer two-dimensional polymers assisted by surfactant monolayers, *Nat. Chem.*, 2019, **11**, 994–1000.

51 T. Zhang, H. Qi, Z. Liao, Y. D. Horev, L. A. Panes-Ruiz, P. S. Petkov, Z. Zhang, R. Shivhare, P. Zhang, K. Liu, V. Bezugly, S. Liu, Z. Zheng, S. Mannsfeld, T. Heine, G. Cuniberti, H. Haick, E. Zschech, U. Kaiser, R. Dong and X. Feng, Engineering crystalline quasi-two-dimensional polyaniline thin film with enhanced electrical and chemiresistive sensing performances, *Nat. Commun.*, 2019, **10**, 4225.

52 A. Prasoon, X. Yu, M. Hambach, D. Bodesheim, K. Liu, A. Zacarias, N. N. Nguyen, T. Seki, A. Dianat, A. Croy, G. Cuniberti, P. Fontaine, Y. Nagata, S. C. B. Mannsfeld, R. Dong, M. Bonn and X. Feng, Site-selective chemical reactions by on-water surface sequential assembly, *Nat. Commun.*, 2023, **14**, 8313.

53 H. Sahabudeen, H. Qi, M. Ballabio, M. Položij, S. Olthof, R. Shivhare, Y. Jing, S. Park, K. Liu, T. Zhang, J. Ma, B. Rellinghaus, S. Mannsfeld, T. Heine, M. Bonn, E. Cánovas, Z. Zheng, U. Kaiser, R. Dong and X. Feng, Highly Crystalline and Semiconducting Imine-Based Two-Dimensional Polymers Enabled by Interfacial Synthesis, *Angew. Chem., Int. Ed.*, 2020, **59**, 6028–6036.

54 Z. Wang, Z. Zhang, H. Qi, A. Ortega-Guerrero, L. Wang, K. Xu, M. Wang, S. Park, F. Hennersdorf, A. Dianat, A. Croy, H. Komber, G. Cuniberti, J. J. Weigand, U. Kaiser, R. Dong and X. Feng, On-water surface synthesis of charged two-dimensional polymer single crystals via the irreversible Katsiritsky reaction, *Nat. Synth.*, 2022, **1**, 69–76.

55 Y. Yang, D. Sabaghi, C. Liu, A. Dianat, D. Mücke, H. Qi, Y. Liu, M. Hambach, Z.-K. Xu, M. Yu, G. Cuniberti, S. C. B. Mannsfeld, U. Kaiser, R. Dong, Z. Wang and X. Feng, On-Water Surface Synthesis of Vinylene-Linked Cationic Two-Dimensional Polymer Films as the Anion-Selective Electrode Coating, *Angew. Chem., Int. Ed.*, 2024, **63**, e202316299.

56 F. Tan, S. Han, D. Peng, H. Wang, J. Yang, P. Zhao, X. Ye, X. Dong, Y. Zheng, N. Zheng, L. Gong, C. Liang, N. Frese, A. Götzhäuser, H. Qi, S. Chen, W. Liu and Z. Zheng, Nanoporous and Highly Thermal Conductive Thin Film of



Single-Crystal Covalent Organic Frameworks Ribbons, *J. Am. Chem. Soc.*, 2021, **143**, 3927–3933.

57 Z. Ou, B. Liang, Z. Liang, F. Tan, X. Dong, L. Gong, P. Zhao, H. Wang, Y. Zou, Y. Xia, X. Chen, W. Liu, H. Qi, U. Kaiser and Z. Zheng, Oriented Growth of Thin Films of Covalent Organic Frameworks with Large Single-Crystalline Domains on the Water Surface, *J. Am. Chem. Soc.*, 2022, **144**, 3233–3241.

58 Y. Yang, B. Liang, J. Kreie, M. Hambach, Z. Liang, C. Wang, S. Huang, X. Dong, L. Gong, C. Liang, D. Lou, Z. Zhou, J. Lu, Y. Yang, X. Zhuang, H. Qi, U. Kaiser, S. C. B. Mannsfeld, W. Liu, A. Gölzhäuser and Z. Zheng, Elastic films of single-crystal two-dimensional covalent organic frameworks, *Nature*, 2024, **630**, 878–883.

59 H. Wang, D. Wu, K. Chen, N. Gu, Y. Chen and B. Zhang, Self-Template Hydrothermal Synthesis of Vinylene-Linked Covalent Organic Framework Nanosheets Confined at the Molecule/Water Interface for an Organic Memristor, *ACS Mater. Lett.*, 2024, **6**, 3376–3383.

60 Z. Zhang and Y. Xu, Hydrothermal Synthesis of Highly Crystalline Zwitterionic Vinylene-Linked Covalent Organic Frameworks with Exceptional Photocatalytic Properties, *J. Am. Chem. Soc.*, 2023, **145**, 25222–25232.

61 T. Kim, S. H. Joo, J. Gong, S. Choi, J. H. Min, Y. Kim, G. Lee, E. Lee, S. Park, S. K. Kwak, H.-S. Lee and B.-S. Kim, Geomimetic Hydrothermal Synthesis of Polyimide-Based Covalent Organic Frameworks, *Angew. Chem., Int. Ed.*, 2022, **61**, e202113780.

62 J. He, B. Luo, H. Zhang, Z. Li, N. Zhu, F. Lan and Y. Wu, Surfactant-free synthesis of covalent organic framework nanospheres in water at room temperature, *J. Colloid Interface Sci.*, 2022, **606**, 1333–1339.

63 X. Kong, Z. Wu, M. Strømme and C. Xu, Ambient Aqueous Synthesis of Imine-Linked Covalent Organic Frameworks (COFs) and Fabrication of Freestanding Cellulose Nanofiber@COF Nanopapers, *J. Am. Chem. Soc.*, 2024, **146**, 742–751.

64 J.-f. Feng, T.-F. Liu and R. Cao, An Electrochromic Hydrogen-Bonded Organic Framework Film, *Angew. Chem., Int. Ed.*, 2020, **59**, 22392–22396.

65 J. M. Rotter, S. Weinberger, J. Kampmann, T. Sick, M. Shalom, T. Bein and D. D. Medina, Covalent Organic Framework Films through Electrophoretic Deposition—Creating Efficient Morphologies for Catalysis, *Chem. Mater.*, 2019, **31**, 10008–10016.

66 R. Wang, Y. Zhou, Y. Zhang, J. Xue, J. Caro and H. Wang, Ultrathin Covalent Organic Framework Membranes Prepared by Rapid Electrophoretic Deposition, *Adv. Mater.*, 2022, **34**, 2204894.

67 X. Wang, J. Yang, X. Shi, Z. Zhang, C. Yin and Y. Wang, Electrosynthesis of Ionic Covalent Organic Frameworks for Charge-Selective Separation of Molecules, *Small*, 2022, **18**, 2107108.

68 M. Wang, Y. Wang, J. Zhao, J. Zou, X. Liang, Z. Zhu, J. Zhu, H. Wang, Y. Wang, F. Pan and Z. Jiang, Electrochemical Interfacial Polymerization toward Ultrathin COF Membranes for Brine Desalination, *Angew. Chem., Int. Ed.*, 2023, **62**, e202219084.

69 Y.-A. Wang, Q. Wu, X. Wang, M. Jiang, R. Zhang, X.-J. Chen, R.-P. Liang and J.-D. Qiu, *In Situ* Electrochemical Interfacial Polymerization for Covalent Organic Frameworks with Tunable Electrochromism, *Angew. Chem., Int. Ed.*, 2024, **63**, e202413071.

70 T. Shirokura, T. Hirohata, K. Sato, E. Villani, K. Sekiya, Y.-A. Chien, T. Kurioka, R. Hifumi, Y. Hattori, M. Sone, I. Tomita and S. Inagi, Site-Selective Synthesis and Concurrent Immobilization of Imine-Based Covalent Organic Frameworks on Electrodes Using an Electrogenerated Acid, *Angew. Chem., Int. Ed.*, 2023, **62**, e202307343.

71 X. Wei, M. Bi, Q. Lou, D. Di, B. Liu and D. Pei, Fast and facile sonochemical fabrication of covalent organic frameworks in water for the adsorption of flavonoids: adsorption behaviors and mechanisms, *Colloids Surf., A*, 2024, **702**, 134731.

72 K. Duan, J. Wang, Y. Zhang and J. Liu, J. Covalent organic frameworks (COFs) functionalized mixed matrix membrane for effective CO<sub>2</sub>/N<sub>2</sub> separation, *Membr. Sci.*, 2019, **572**, 588–595.

73 Q. Wang, L. Gao, P. Wang, Y. Wang, Y. Xu, H. Xu, X. Wang, Z. Meng and K. Xi, Preparation of sp<sup>2</sup> carbon-bonded π-conjugated COF aerogels by ultrasound-assisted mild solvothermal reaction for multi-functional applications, *Nanoscale*, 2024, **16**, 15298–15307.

74 S.-T. Yang, J. Kim, H.-Y. Cho, S. Kim and W.-S. Ahn, Facile synthesis of covalent organic frameworks COF-1 and COF-5 by sonochemical method, *RSC Adv.*, 2012, **2**, 10179–10181.

75 W. Zhao, P. Yan, H. Yang, M. Bahri, A. M. James, H. Chen, L. Liu, B. Li, Z. Pang, R. Clowes, N. D. Browning, J. W. Ward, Y. Wu and A. I. Cooper, Using sound to synthesize covalent organic frameworks in water, *Nat. Synth.*, 2022, **1**, 87–95.

76 W. Zhao, P. Yan, B. Li, M. Bahri, L. Liu, X. Zhou, R. Clowes, N. D. Browning, Y. Wu, J. W. Ward and A. I. Cooper, Accelerated Synthesis and Discovery of Covalent Organic Framework Photocatalysts for Hydrogen Peroxide Production, *J. Am. Chem. Soc.*, 2022, **144**, 9902–9909.

77 C. J. F. Oliveira, S. K. S. Freitas, I. G. P. P. de Sousa, P. M. Esteves and R. A. Simao, Solvent role on covalent organic framework thin film formation promoted by ultrasound, *Colloids Surf., A*, 2020, **585**, 124086.

78 S. Wang, Y. Yang, H. Zhang, Z. Zhang, C. Zhang, X. Huang, D. Kozawa, P. Liu, B.-G. Li and W.-J. Wang, Toward Covalent Organic Framework Metastructures, *J. Am. Chem. Soc.*, 2021, **143**, 5003–5010.

79 T. Huang, H. Jiang, J. C. Douglan, Y. Chen, S. Yin, J. Zhang, X. Deng, H. Wu, Y. Yin, D. R. Dekel, M. D. Guiver and Z. Jiang, Single Solution-Phase Synthesis of Charged Covalent Organic Framework Nanosheets with High Volume Yield, *Angew. Chem., Int. Ed.*, 2023, **62**, e202209306.

80 R.-J. Wei, M. Xie, R.-Q. Xia, J. Chen, H.-J. Hu, G.-H. Ning and D. Li, Gold(I)-Organic Frameworks as Catalysts for Carboxylation of Alkynes with CO<sub>2</sub>, *J. Am. Chem. Soc.*, 2023, **145**, 22720–22727.



81 J.-C. Wang, T. Sun, J. Zhang, Z. Chen, J.-Q. Du, J.-L. Kan and Y.-B. Dong, Construction of covalent organic frameworks *via* the Mannich reaction at room temperature for light-driven oxidative hydroxylation of arylboronic acids, *Chemi. Sci.*, 2024, **15**, 18634–18639.

82 B. P. Biswal, S. Chandra, S. Kandambeth, B. Lukose, T. Heine and R. Banerjee, Mechanochemical Synthesis of Chemically Stable Isoreticular Covalent Organic Frameworks, *J. Am. Chem. Soc.*, 2013, **135**, 5328–5331.

83 G. Das, D. Balaji Shinde, S. Kandambeth, B. P. Biswal and R. Banerjee, Mechanosynthesis of imine,  $\beta$ -ketoenamine, and hydrogen-bonded imine-linked covalent organic frameworks using liquid-assisted grinding, *Chem. Commun.*, 2014, **50**, 12615–12618.

84 K. Asokan, M. K. Patil, S. P. Mukherjee, S. B. Sukumaran and T. Nandakumar, Scalable Mechanochemical Synthesis of  $\beta$ -Ketoenamine-linked Covalent Organic Frameworks for Methane Storage, *Chem.-Asian J.*, 2022, **17**, e202201012.

85 M. Zhang, J. Chen, S. Zhang, X. Zhou, L. He, M. V. Sheridan, M. Yuan, M. Zhang, L. Chen, X. Dai, F. Ma, J. Wang, J. Hu, G. Wu, X. Kong, R. Zhou, T. E. Albrecht-Schmitt, Z. Chai and S. Wang, Electron Beam Irradiation as a General Approach for the Rapid Synthesis of Covalent Organic Frameworks under Ambient Conditions, *J. Am. Chem. Soc.*, 2020, **142**, 9169–9174.

86 M. Zhang, M. Yuan, X. Zhao, J. Chen, L. He, Q. Gao, J. Hu, G. Wu, Z. Chai and S. Wang, Radiation-induced one-pot synthesis of grafted covalent organic frameworks, *Sci. China Chem.*, 2023, **66**, 1781–1787.

87 A. M. Elewa, I. M. A. Mekhemer, A. F. M. El-Mahdy, A. Sabbah, S.-Y. Chen, L.-Y. Ting, S. Abdelnaser and H.-H. Chou, Room-Temperature Synthesis of Covalent Organic Frameworks using Gamma-Irradiation in Open-Air Conditions, *Small*, 2024, **20**, 2311472.

88 S. Kim, C. Park, M. Lee, I. Song, J. Kim, M. Lee, J. Jung, Y. Kim, H. Lim and H. C. Choi, Rapid Photochemical Synthesis of Sea-Urchin-Shaped Hierarchical Porous COF-5 and Its Lithography-Free Patterned Growth, *Adv. Funct. Mater.*, 2017, **27**, 1700925.

89 C.-J. Wu, X.-Y. Li, T.-R. Li, M.-Z. Shao, L.-J. Niu, X.-F. Lu, J.-L. Kan, Y. Geng and Y.-B. Dong, Natural Sunlight Photocatalytic Synthesis of Benzoxazole-Bridged Covalent Organic Framework for Photocatalysis, *J. Am. Chem. Soc.*, 2022, **144**, 18750–18755.

90 G.-B. Wang, Y.-J. Wang, J.-L. Kan, K.-H. Xie, H.-P. Xu, F. Zhao, M.-C. Wang, Y. Geng and Y.-B. Dong, Construction of Covalent Organic Frameworks *via* a Visible-Light-Activated Photocatalytic Multicomponent Reaction, *J. Am. Chem. Soc.*, 2023, **145**, 4951–4956.

91 A. Acharjya, P. Pachfule, J. Roeser, F.-J. Schmitt and A. Thomas, Vinylene-Linked Covalent Organic Frameworks by Base-Catalyzed Aldol Condensation, *Angew. Chem., Int. Ed.*, 2019, **58**, 14865–14870.

92 C. Sun, J. J. Oppenheim, G. Skorupskii, L. Yang and M. Dincă, Reversible topochemical polymerization and depolymerization of a crystalline 3D porous organic polymer with C-C bond linkages, *Chem.*, 2022, **8**, 3215–3224.

93 N. Huang, X. Ding, J. Kim, H. Ihee and D. Jiang, A Photoresponsive Smart Covalent Organic Framework, *Angew. Chem., Int. Ed.*, 2015, **54**, 8704–8707.

94 T. Jadhav, Y. Fang, C.-H. Liu, A. Dadvand, E. Hamzehpoor, W. Patterson, A. Jonderian, R. S. Stein and D. F. Perepichka, Transformation between 2D and 3D Covalent Organic Frameworks *via* Reversible [2 + 2] Cycloaddition, *J. Am. Chem. Soc.*, 2020, **142**, 8862–8870.

95 T. Kim, J. Oh, S. C. Kim, J.-G. Ahn, S. Kim, Y. Y. Kim and H. Lim, Photochemical and Patternable Synthesis of 2D Covalent Organic Framework Thin Film Using Dynamic Liquid/Solid Interface, *Small Methods*, 2024, 2400063, DOI: [10.1002/smtb.202400063](https://doi.org/10.1002/smtb.202400063).

